

Supplementary Information

Enhanced Electromagnetic Wave Absorption of Magnetic Co Nanoparticles/CNTs/EG Porous Composites with Waterproof, Flame-retardant and Thermal Management Functions

Zhen Xiang, Xiaojie Zhu, YanYan Dong, Xiang Zhang, Yuyang Shi, and Wei Lu*

Shanghai Key Lab. of D&A for Metal-Functional Materials, School of Materials
Science & Engineering, Tongji University, Shanghai 201804, China.

*Corresponding authors: Wei Lu, E-mail: weilu@tongji.edu.cn

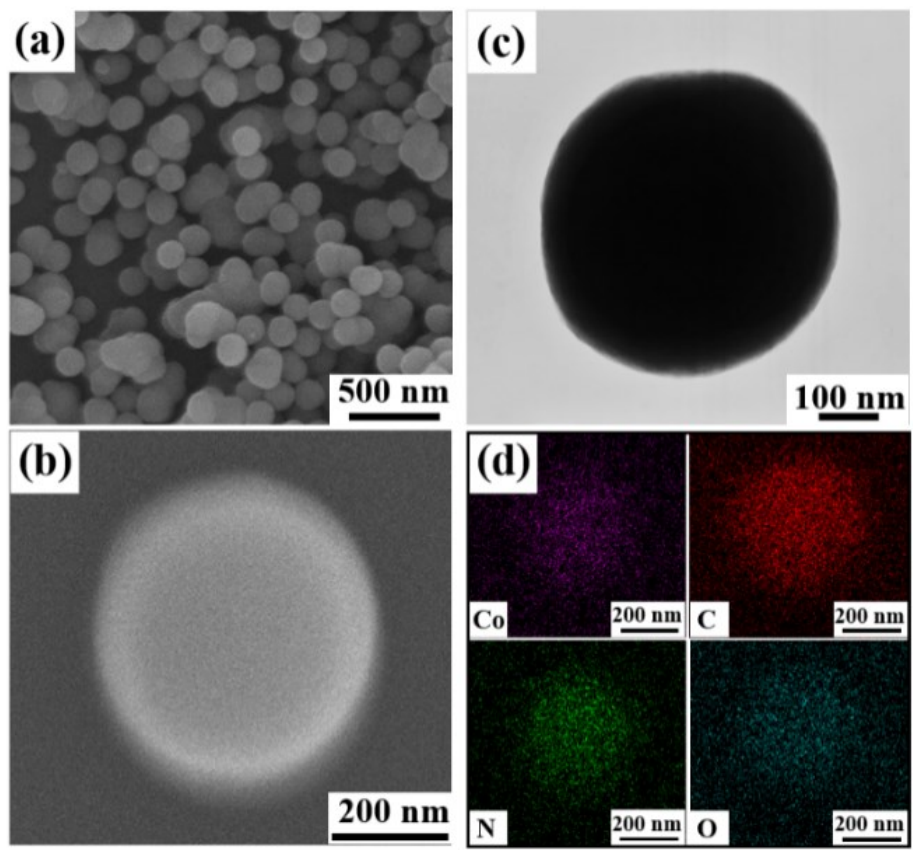


Figure S1 SEM images of (a) Co-MOFs particles, (b) a single Co-MOFs particle, (c) TEM image of Co-MOFs particle, and (d) EDS mapping of Co-MOFs particle.

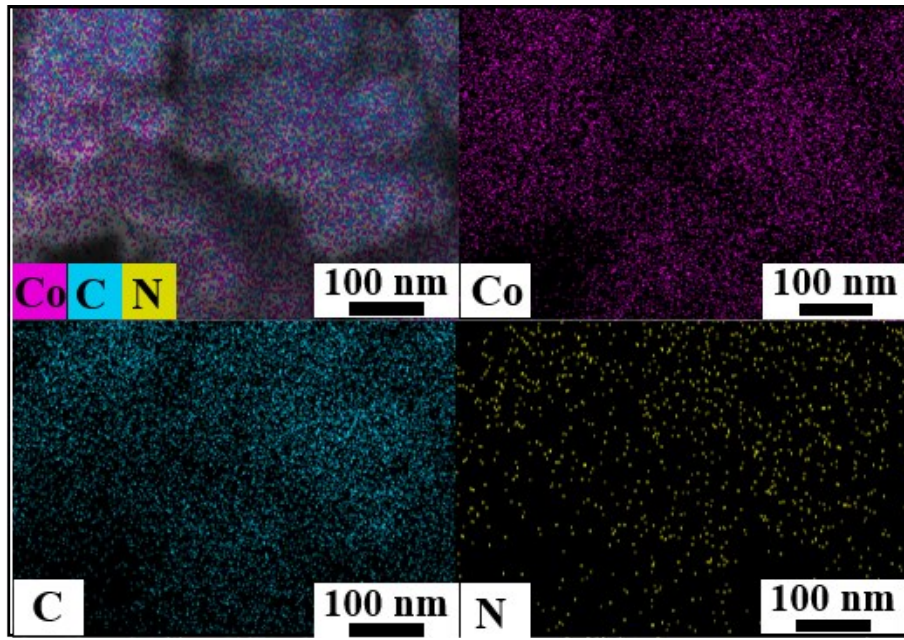


Figure S2 The EDS mapping of Co/CNTs nanocomposites.

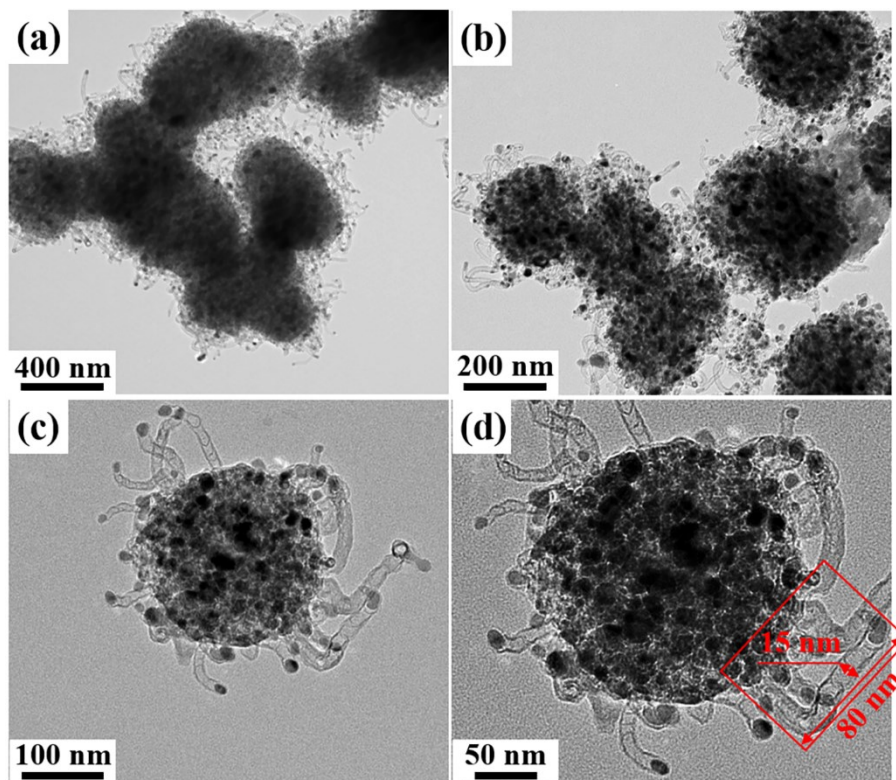


Figure S3 TEM images of Co/CNTs nanocomposites.

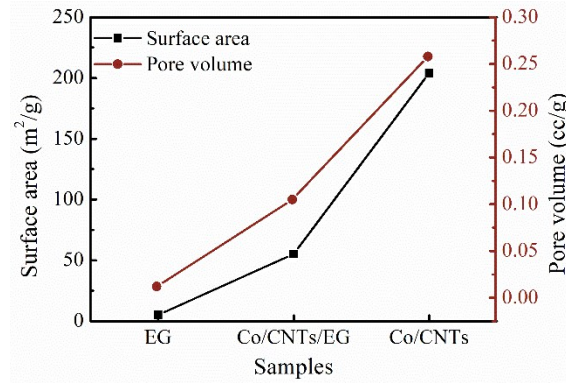


Figure S4 The surface area and total pore volume of samples.

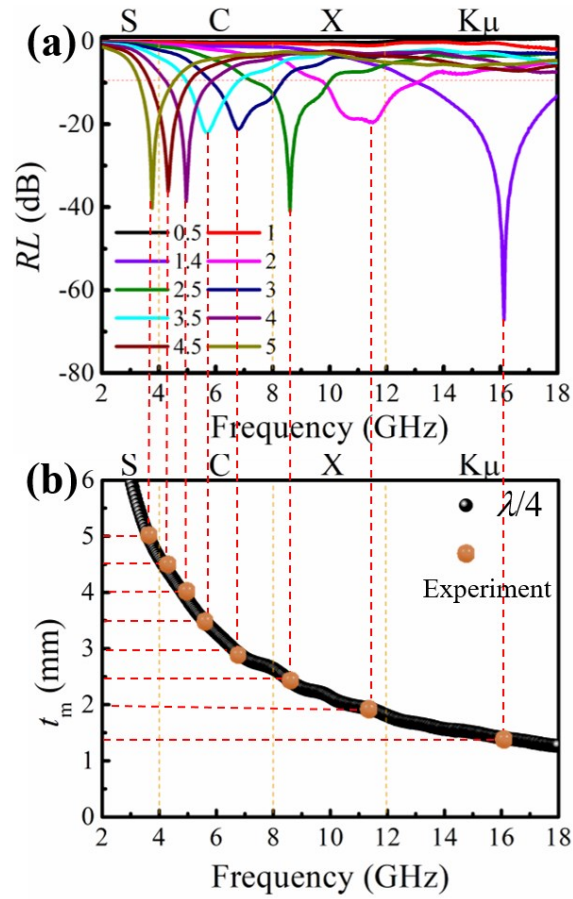


Figure S5 (a) RL values versus frequency and thicknesses, (b) The relationship between simulated matching thickness t_m and peak frequency of Co/CNTs/EG_(4:3) nanocomposites.

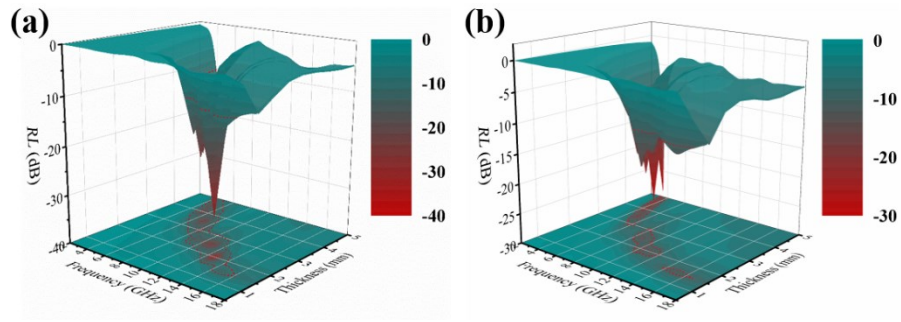


Figure S6 3D representations of RL values for (a) Co/CNTs/EG_(2:1) and (b) Co/CNTs/EG_(1:1).

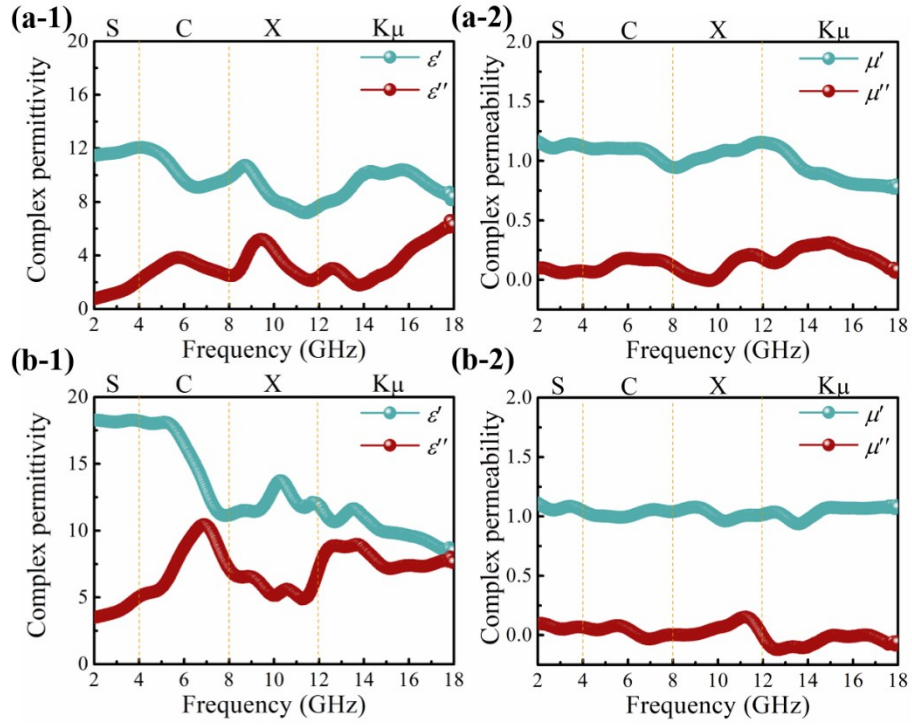


Figure S7 The frequency dependence of permittivity (ϵ' , ϵ'') and permeability (μ' , μ'') of Co/CNTs/EG_(2:1) (a-1, a-2) and Co/CNTs/EG_(1:1) (b-1, b-2).

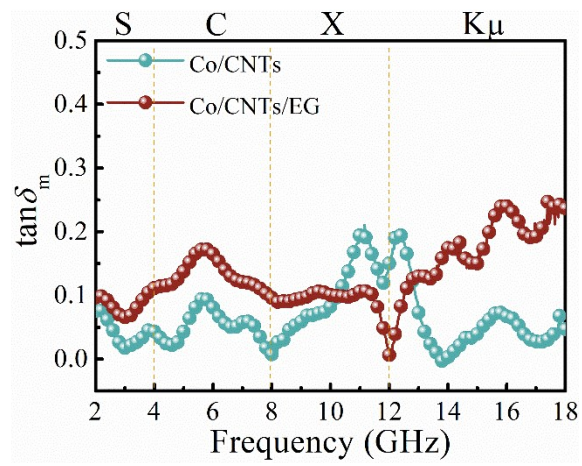


Figure S8 The frequency dependence of magnetic loss tangent ($\tan\delta_m$) of Co/CNTs and Co/CNTs/EG_(4:3).

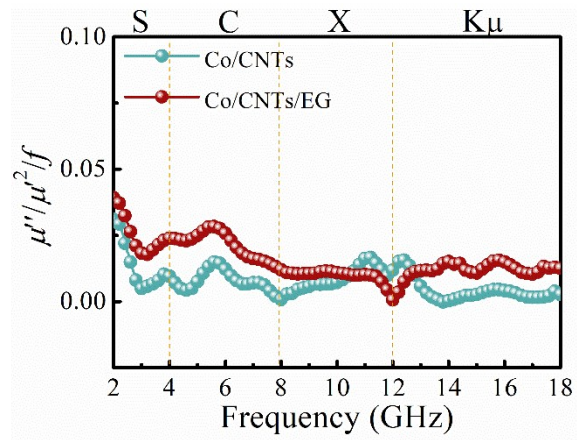


Figure S9 The frequency-dependent $\mu''(\mu')^{-2}f^1$ values of Co/CNTs and Co/CNTs/EG_(4:3).